



Exploration of cell-cell interactions and the notch signaling pathway in the gonadal niche of *Crassostrea gigas*

Huihui Wang^a, Hong Yu^{a,b,*}, Qi Li^{a,b,c}

^a Key Laboratory of Mariculture (Ocean University of China), Ministry of Education, Qingdao 266003, China

^b Laboratory for Marine Fisheries Science and Food Production Processes, Qingdao National Laboratory for Marine Science and Technology, Qingdao 266237, China

^c Laboratory of Tropical Marine Germplasm Resources and Breeding Engineering, Sanya Oceanographic Institution, Ocean University of China, Sanya 572000, China

ARTICLE INFO

Editor by: Michael Hedrick

Keywords:

Gonadal niche
Notch signaling pathway
Desmosome-like
Crassostrea gigas

ABSTRACT

The Notch signaling pathway plays a pivotal role in governing cell fate determinations within the gonadal niche. This study provides an extensive elucidation of the male and female gonadal niches within *Crassostrea gigas*. Examination via transmission electron microscopy revealed the presence of desmosome-like connection not only between germ cells and niche cells but also among adjacent niche cells within the oyster gonad. Transcriptomic analysis identified several putative Notch pathway components, including *CgJAG1*, *CgNOTCH1*, *CgSuh*, and *CgHey1*. Phylogenetic analysis indicated a close evolutionary relationship between *CgJAG1*, *CgNOTCH1*, and *CgHey1* and Notch members present in *Drosophila*. Expression profiling results indicated a notable abundance of *CgHey1* in the gonads, while *CgJAG1* and *CgNOTCH1* displayed distinct expression patterns associated with sexual dimorphism. *In situ* hybridization findings corroborated the predominant expression of *CgJAG1* in male niche cells, while *CgNOTCH1* was expressed in both male and female germ cells, as well as female niche cells. These findings demonstrate the important role of the Notch signaling pathway in the gonadal niche of oysters.

1. Introduction

Gametogenesis is a crucial aspect of development, with the gonadal niche being a central focal point. This specialized environment supports the growth and development of germ cells by providing regulatory factors and signaling molecules that coordinate their precise maturation. In human females, granulosa cells activate the BMP signaling pathway to regulate the transition from mitosis to meiosis in fetal germ cells (Li et al., 2017). Disrupting somatic cell function in male *Drosophila* leads to an imbalance between germline cell renewal and differentiation (Kiger et al., 2000). Moreover, Sertoli cells serve as a protective barrier, shielding germ cells from undesired cellular interactions (McIntyre and Nance, 2020). Somatic cells are present in cysts of fish, providing structural support and nutrition to developing germ cells (Mazzoni et al., 2010). In various animal species, the formation of the gonadal niche relies on adhesion molecules, including components of desmosomes which facilitate cell adhesion (Piprek et al., 2017). Previous studies on the gonadal microenvironment of bivalves have predominantly concentrated on descriptive analyses of niche cells within the gonads. In *Pitar rudis* and *Chamelea gallina*, the asymmetrically formed Sertoli cells

extended from the basal lamina into the lumen, enclosing germ cells (Erkan and Sousa, 2002). In the testes of the mussel *Modiolus kurilensis*, the cytoplasm of the accessory cells was less electron dense than that of the neighboring germ cells (Yurchenko and Vaschenko, 2010). Pleomorphic and amoeboid accessory cells (intragonadal somatic cells) were found in the testes of *Crassostrea gigas* (Franco et al., 2011; Kim et al., 2010). However, functional role of bivalve gonadal niche cells remains to be elucidated.

One important signaling pathway in the gonadal niche, initially discovered in *Drosophila*, is the Notch signaling pathway (Artavanis-Tsakonas et al., 1995). This pathway primarily involves four receptors: *Notch1*, *Notch2*, *Notch3*, and *Notch4*, with ligands encoded by *JAG1*, *JAG2*, *DLL1*, *DLL3*, and *DLL4* genes. In *Drosophila*, these ligands are encoded by the *Delta* and *Serrate* genes (Kitadate and Kobayashi, 2010; Vanorny and Mayo, 2017). The binding of ligands and receptors initiates intracellular cleavage of the receptor, allowing the entry of the Notch intracellular structural domains (NICD) into the nucleus. NICD subsequently interacts with the DNA-binding protein SUH, forming a complex that triggers the transcription of Notch target genes, including members of the Hes/Hey family (Borggreffe and Oswald, 2009). In mammals, the

* Corresponding author at: Key Laboratory of Mariculture, Ministry of Education, Ocean University of China, Qingdao, China.

E-mail address: hongyu@ouc.edu.cn (H. Yu).

huihui_wang12707 (H. Wang)

<https://doi.org/10.1016/j.cbpa.2024.111639>

Received 10 December 2023; Received in revised form 13 April 2024; Accepted 14 April 2024

Available online 17 April 2024

1095-6433/© 2024 Elsevier Inc. All rights reserved.

delta ligands are expressed in granulosa cells, whereas the receptor genes and target genes are expressed in oocytes. Notch transduction has been implicated in follicle assembly (Feng et al., 2014). In the *Drosophila* testis, the *Serrate* ligand, expressed in somatic gonadal precursors, activates Notch, inducing the differentiation of hub cells (Kitadate and Kobayashi, 2010). Additionally, the inhibition of Notch signaling has been observed to impair gonadal development and sexual differentiation in carp fish (Jia et al., 2018). When compared to other bivalves, such as scallops, the gonadal organs of *C. gigas* are diffuse and episodic. This unique characteristic urges us to examine the role of the gonad micro-environment in oyster gonad development. Despite many studies the reproduction of *C. gigas*, largely due to its commercial value and captivating gender determination patterns, the signal transduction within the gonadal niche was never, to our knowledge, reported.

Our study observed structures where germ cells and niche cells directly interact. Additionally, we identified and characterized potential members of the Notch signaling pathway that may contribute to the oyster gonadal niche. Overall, our study provides valuable insights into the distinctive features of the diffuse gonadal microenvironment in marine invertebrates.

2. Materials and methods

2.1. Sample collection and histological identification

Monthly collections of adult Pacific oysters, aged two years, were obtained from Sanggou Bay, Shandong, China. A total of six different tissues were sampled, including gonad, mantle, gill, labial palp, adductor muscle and digestive gland. Tissues intended for RNA isolation were carefully stored at a freezing temperature of -80°C . To visualize the sex and gonadal developmental stage of the oysters, gonadal samples were first immersed in Bouin's solution for 12 h. They were then transferred to 70% ethanol, washed with xylene, and eventually embedded in paraffin. Subsequently, the paraffin-embedded samples were cut into thin tissue sections, approximately $5\ \mu\text{m}$ in thickness, using Leica RM 2016 rotary microtome (Leica, Germany). The sections were stained with H&E and observed using an Olympus BX53 microscope (Olympus, Japan). Concomitantly, the gonad was subjected to 4% paraformaldehyde at a temperature of 4°C overnight, and stored in methanol at -20°C for subsequent *in situ* hybridization analysis.

2.2. Transmission electron microscopy (TEM) sample preparation

In order to conduct TEM analysis, male and female oyster gonadal samples were collected at stage II. Subsequently, small tissue fragments (about $1\ \text{mm}^3$) were pre-fixed with a 2.5% glutaraldehyde solution (EMS). The ultrastructure analysis of the tissues followed the protocol established by Li et al. (2022).

2.3. RNA isolation and cDNA synthesis

Standard protocols were employed to extract the total RNA utilizing TRIzol reagent. The concentration of RNA was determined using a Nanodrop spectrophotometer (Thermo Fisher Scientific, USA). Assessment of RNA purity involved measurement of the absorbance ratio exceeding 1.8 at 260/280 nm. Integrity evaluation was conducted through observing the results on a 1% agarose gel. Subsequently, reverse transcription was conducted applying the Evo M-MLV RT kit (Accurate Biotechnology, China).

2.4. Bioinformatics analysis of NOTCH signaling pathway members

The whole genome peptide sequence dataset of *C. gigas* was downloaded from the oyster genome (GCF_902806645.1, Feb 19, 2020; *Crassostrea gigas* genome assembly cgigas_uk_roslin_v1 - NCBI - NLM (nih.gov)). Protein sequences of ligands, receptors, Suh, and target genes

associated with the Notch signaling pathway were collected from various organisms. These organisms include *Homo sapiens*, *Mus musculus*, *Drosophila melanogaster*, *Danio rerio*, *Caenorhabditis elegans*, and *Xenopus laevis*. The protein sequences were downloaded from NCBI (<https://www.ncbi.nlm.nih.gov/>) or UniProt (<https://www.uniprot.org/>) and were used to assemble the initial reference sequence set. We first aligned the seed protein sequences for each gene family using MAFFT (v 7.520-1), and saved the alignment output as *.fasta files (Katoh and Standley, 2013). HMMER (v 3.3.2) with default parameters was used to screen related gene families, using the family specific *.fasta alignment file as input for hmmbuild script. Afterwards, the seed sequences were subjected to BLASTP searches against the oyster genome with the e-value threshold below $1e-5$. The protein sequences identified from the HMMER analysis were compared to the proteins identified through BLAST to generate a gene family specific non-redundant gene list. The Conserved Domain Database (CDD, <https://www.ncbi.nlm.nih.gov/cdd/>) was used to confirm and ensure that all candidate genes contained the conserved domains. Alignments created with the L-INS-I method of MAFFT were trimmed with trimAL (v1.4.rev15, -gt 0.9), and phylogenies were inferred with raxmlHPC-PTHREADS-SSE3 (v 8.2.12) of RAxML (Stamatakis, 2014). One thousand bootstraps were used to assess the significance of the phylogenetic tree, and the model of amino acid substitution PROT-GAMMAILG was applied. To predict the subcellular localization, we utilized Cell-PLoc 2.0 (<http://www.csbio.sjtu.edu.cn/bioinf/Cell-PLoc-2/>) (Chou and Shen, 2010). Signal peptides and transmembrane domains of ligands and receptors were predicted using the SignalP 5.0 Server (SignalP 5.0 - DTU Health Tech - Bioinformatic Services) and the TMHMM Server v. 2.0 (TMHMM 2.0 - DTU Health Tech - Bioinformatic Services), respectively (Almagro Armenteros et al., 2019). Transcriptomic data of diploid gonads and tissues of *C. gigas* were downloaded (accession number: SRP112367; GSE31012). The tissue and diploid developmental gonad transcriptome data were processed according to Yue et al. (2018). The gene expression heatmap was generated using the OmicShare tools available at www.omicshare.com/tools.

2.5. Quantitative real-time PCR (qPCR)

The qPCR amplification was generated with Premix Pro Taq HS QPCR kit (Accurate Biotechnology, China) on a LightCycler 480 II detection system (Roche, Switzerland) according to the instructions of manufacturer. Primer pairs were listed in Table 1. The amplified region spans intron(s). To determine the PCR efficiency of each primer pair, the standard curve method was employed, using five points of cDNA serial dilutions. The cDNA was diluted 25-fold and analyzed by qPCR for *CgJAG1* (LOC105317836), *CgNOTCH1* (LOC105344250), *CgSuh* (LOC105337369) and *CgHey1* (LOC105341723). For qPCR analysis, a minimum of three biological replicates were used for each gene, with at least two technical replicates analyzed for each biological replicate. Three commonly used housekeeping genes in *C. gigas*, *Ef1*, *GAPDH*, and *Actin* were selected as candidate reference genes (Farcy et al., 2009). Their suitability for normalization was assessed using the Normfinder Excel Add-in (<https://moma.dk/normfinder-software>). Among them, *Ef1* exhibited the highest stability value (0.281), leading us to select it as the reference gene (Table S1). The relative expression levels were determined using the $2^{-\Delta\Delta\text{Ct}}$ method.

2.6. In situ hybridization (ISH) and immunohistochemistry

In situ hybridization was conducted based on previously established protocol with slight modifications (Yue et al., 2021). In brief, specific cDNA segments of *CgJAG1B* and *CgNOTCH1* were amplified using primers containing T7 promoter sequences (Table 1). After sequence confirmation, sense and antisense riboprobes with digoxigenin labels were synthesized using a DIG RNA labelling kit (Roche, Germany). The diploid male and female gonad samples of various developmental stages

Table 1
Primers used in this study.

Name	Primers (5'-3')	Purpose	Amplicon (bp)	Amplification efficiencies (%)	R ² value	
qCgJAG1B RT F	CTGCCCAAAGTCAGAGGCA	qPCR	335	108.7	0.9975	
qCgJAG1B RT R	CGAATCTGATCGCCCACTGA					
qCgNOTCH1 RT F	TTGGTITTTGGACACACAAGGTTTC		164	90.8	0.9389	
qCgNOTCH1 RT R	CAGAAATGGGCATCCGGTCCG					
qCgSuh RT F	ACGTGGAAAGTTGCGTACATCG		195	94	0.9741	
qCgSuh RT R	ACACTGTAGGTGTAACCATCTGAG					
qCgHey1 RT F	TGAACGTGGCTCAGGAAGGG		210	108.9	0.9953	
qCgHey1 RT R	CGCCGTTTCTCTATCACCCCA					
ISH CgJAG1 F	GGATGGACAGGGAAGAACT		ISH			
ISH CgJAG1 R	TAATACGACTCACTATAGGGCCACACACATTGGAGGAG					
ISH CgNOTCH1 F	CTGGGATACTCTGGAACCTCT					
ISHCgNOTCH1 R	TAATACGACTCACTATAGGGCACAACGACTATTTCACGCA					

as described below were embedded in paraffin wax. Five-micrometer tissue sections were mounted, dewaxed in xylenes, rehydrated through graded ethanol, and placed in PBS. Slides were immersed in PBS contained 10 µg/ml proteinase K at 37 °C for 5 min, and then covered with a hybridization solution (60% deionized formamide, 7.5% dextran sulfate, 1 × denhard solution, 0.3 M NaCl, 0.02 M Tris-HCl, 0.0025 M EDTA, pH = 8.0) containing 0.1–0.5 ng/µl pooled CgJAG1B or CgNOTCH1 riboprobes and hybridized for 18 h at 65 °C. After washing in 5 × SSC, 2 × SSC, 1 × SSC, and 0.2 × SSC at room temperature for 30 min each, sections were transferred to a washing buffer (0.5 M maleic acid, 0.75 M NaCl, pH = 7.5) containing 0.1% Tween-20. Tissues were blocked in 1% blocking reagent at room temperature (RT) for 2 h, and then incubated with anti-digoxigenin-AP Fab fragments (Roche, Germany). After washing with PBS, the sections were incubated in NBT/BCIP solution. The diploid male and female gonad samples at the growth stage were used for immunohistochemistry. Tissue sections were treated with primary antibody targeting DSG1 (Desmoglein 1) (1:10; Absin), followed by incubation with a secondary antibody using GTVision™ III Detection System/Mo&Rb (including DAB) (GK500705, Gene Tech). The hematoxylin was adopted to visualize the nuclei. An Olympus BX53 microscope coupled with a DP80 camera (Olympus, Japan) was used to analyze the sections and capture images.

2.7. Statistical analysis

Statistical analyses were performed with SPSS 26.0. Differences among the groups were analyzed by one-way ANOVA. A significance level of $P < 0.05$ was considered as significant. Standard error of the mean (SEM) is represented by error bars.

3. Results

3.1. Overview of the oyster gonadal niche

TEM was conducted to investigate the somatic niche within the gonads of both male and female oysters. In the male gonad, spermatogonia, primary spermatocytes characterized by prominent nucleoli, and secondary spermatocytes with chromatin organized in a patchwork pattern were clearly observed (Fig. S1 A, B). Amoeboid niche cells, which exhibited an abundance of vacuoles, a high glycogen content, small mitochondria, and a limited number of lysosomes in the cytoplasm, were observed in close proximity to spermatogonia, primary spermatocytes, secondary spermatocytes (Fig. 1A, B). Importantly, the size of male niche cells exhibited variability (Fig. 1A, B). Additionally, the presence of a phagocytized spermatocyte within cytoplasm of a niche cell was notable (Fig. 1B).

In the female, gonadal niche displayed its own distinctive features. Niche cells were observed surrounding the oogonia and oocytes, extending cytoplasmic processes resembling pseudopodia (Fig. S1C). The oogonia exhibited a high nucleocytoplasmic ratio, with dense nuage surrounding the nucleus, while the oocyte cytoplasm contained a

multitude of endocytotic vesicle-containing yolk granules (Fig. S1C). The cytoplasm of female niche cells showed evident rough endoplasmic reticulum and glycogen particles (Fig. 1C).

We next attempted to investigate the cellular junction between male and female niche cells and germ cells by staining with desmosome component marker DSG1. However, no discernible signals were observed in gonads at the growth stages (Fig. S1D). Subsequently, through TEM, desmosome-like structures were observed at regions of cell membrane contact, both between spermatocytes and male niche cells, and between oogonia, oocytes, and female niche cells (Fig. 1A, C). Surprisingly, desmosome-like structures were also observed between niche cells in both male and female gonads (Fig. 1B, C).

3.2. Sequence and phylogenetic analysis of members in NOTCH signaling pathway

Based on sequence similarity and the presence of conserved structural domains, three Delta ligands, one Notch receptor gene, one DNA-binding protein, and 13 Notch target genes were identified in the oyster genome. The analysis of conserved domains revealed that the identified ligands exhibit the DSL domain (Fig. 2A). Additionally, *CgDLL1.a*, *CgDLL1.b*, and *CgJAG1*, possess one or more EGF_CA domains (Fig. 2A). SignalIP predictions indicated that the Delta ligands contained a signal peptide sequence of approximately 20 amino acids at the N-terminus (Fig. S2A). They also exhibit one or two transmembrane regions (Fig. S2B).

Phylogenetic analysis indicated that the ligands of oysters formed two distinct groups (Jagged and Delta) along with members from other species (Fig. 2B). The ligand *CgJAG1* grouped with high support values in the Jagged clade, while *CgDLL1.a* and *CgDLL1.b* belonged to the Delta clade (Fig. 2B). The ligands from *M. yessoensis*, *M. coruscus*, and *C. gigas* clustered together with *Serrate* of *D. melanogaster*, indicating a closer evolutionary relationship among invertebrates (Fig. 2B).

The analysis of the Notch receptor in oysters showed that *CgNOTCH1* is a single-pass transmembrane receptor protein composed of a signal peptide and classic domains (EGF_CA repeat, Notch, JMTM_dNotch, ANKYR, and ROM1 superfamily) (Fig. 2C, S2). Phylogenetically broad tree evidenced that *CgNOTCH1* was arranged into the invertebrate *NOTCH1* clade (Fig. 2D). Turning to the analysis of putative *CgSuh*, three conserved domains (LAG1-DNA binding, BTB, and IPT_RBP_Jkappa) were identified (Fig. 3A). Phylogenetic evidence confirmed the classification of *CgSuh* within the invertebrate *Suh* clade (Fig. 3B). As for the identification of the primary Notch effectors, the bHLH domain emerged as a conserved feature of the HEY family (Fig. 3C). The Orange domain was annotated in *CgHes1a*, *CgHes1b*, *CgHes4a*, *CgHes4b*, and *CgHey1* (Fig. 3C). Moreover, phylogenetic analysis indicated that members of the HES family in oysters formed a specific clade alongside counterparts from other species (Fig. 3D). Subcellular localization of these genes was also predicted using Cell PLoc 2.0. The results showed that the ligands and receptor were likely located in the extracellular space and on the cell membrane, respectively, while downstream proteins were predicted to

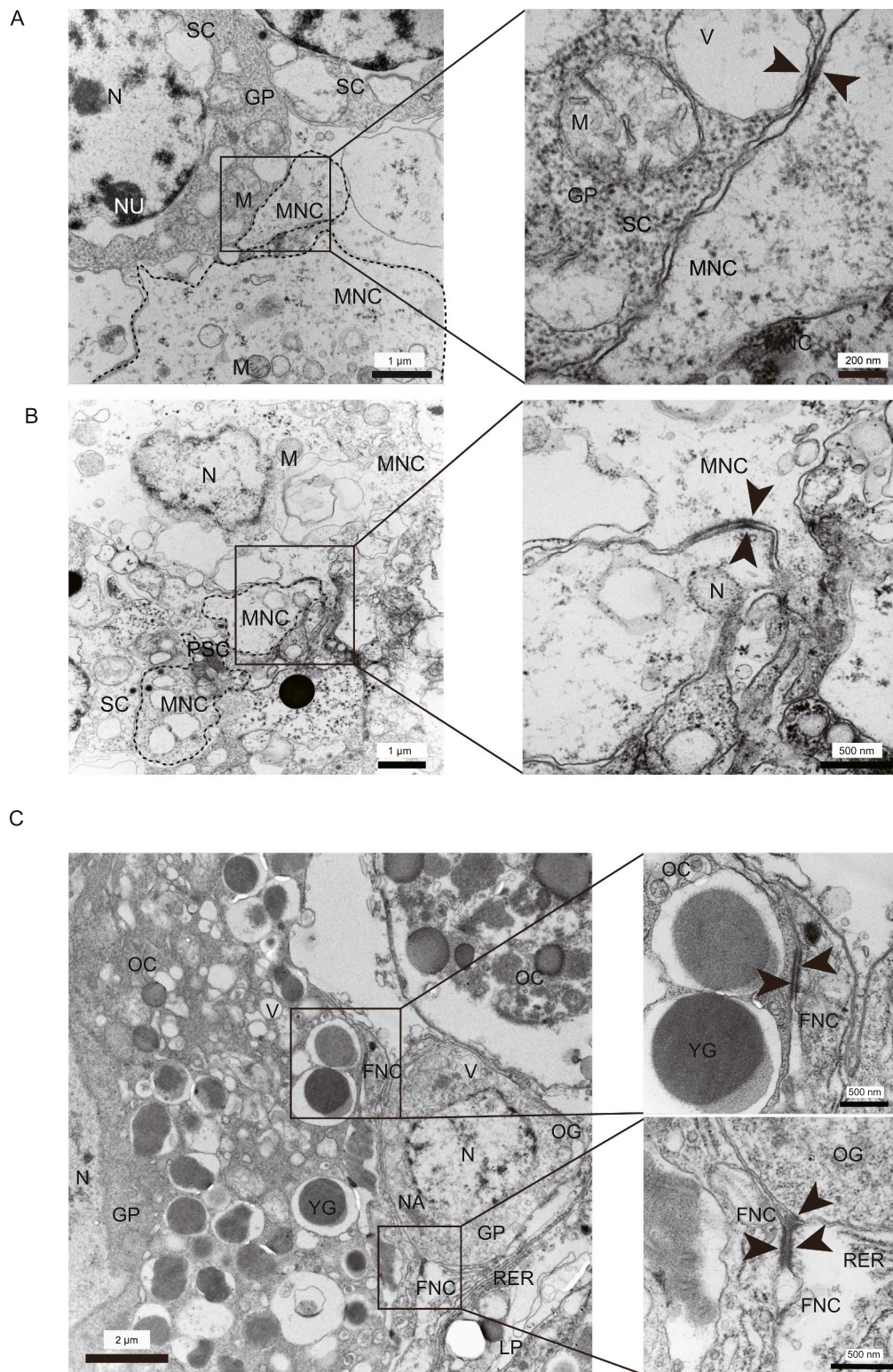


Fig. 1. Morphological organization of the gonadal niche, TEM. (A, B) Overview of the male gonadal niche (left) and a magnified image of the cell connection between spermatocytes (SC) and male niche cells (MNC) (dashed line), as well as between adjacent niche cells (right). Glycogen-rich particle cytoplasm (GP) of spermatocytes (SC) with a round nucleus (N), obvious nucleolus (NU), mitochondria (M), and electron-lucent vacuoles (V). Amoeboid niche cells with an abundance of vacuoles (V) fill the spermatocyte gap. A phagocytosed spermatocyte (PSC) is visible in the cytoplasm of the niche cell. Male niche cells (MNC) connected to each other and to spermatocytes (SC) via desmosome-like contacts (arrowheads). (C) Overview of the female gonadal niche with oogonia (OG), oocytes (OC), and female niche cells (FNC). Oogonia contains nuage (NA) and glycogen particles (GP). Oocytes contain yolk granules (YG) and glycogen particles (GP). The elongated female niche cells (FNC) with rough endoplasmic reticulum (RER) are located between female germ cells. The desmosome-like contacts (arrowheads) are observed between oocyte and niche cell (top right), between oogonia and niche cell, and between neighboring niche cells (bottom right). Scale bars: A (left) = 1 μ m; A (right) = 200 nm; B (left) = 1 μ m; B (right) = 500 nm; C (left) = 2 μ m; C (right) = 500 nm.

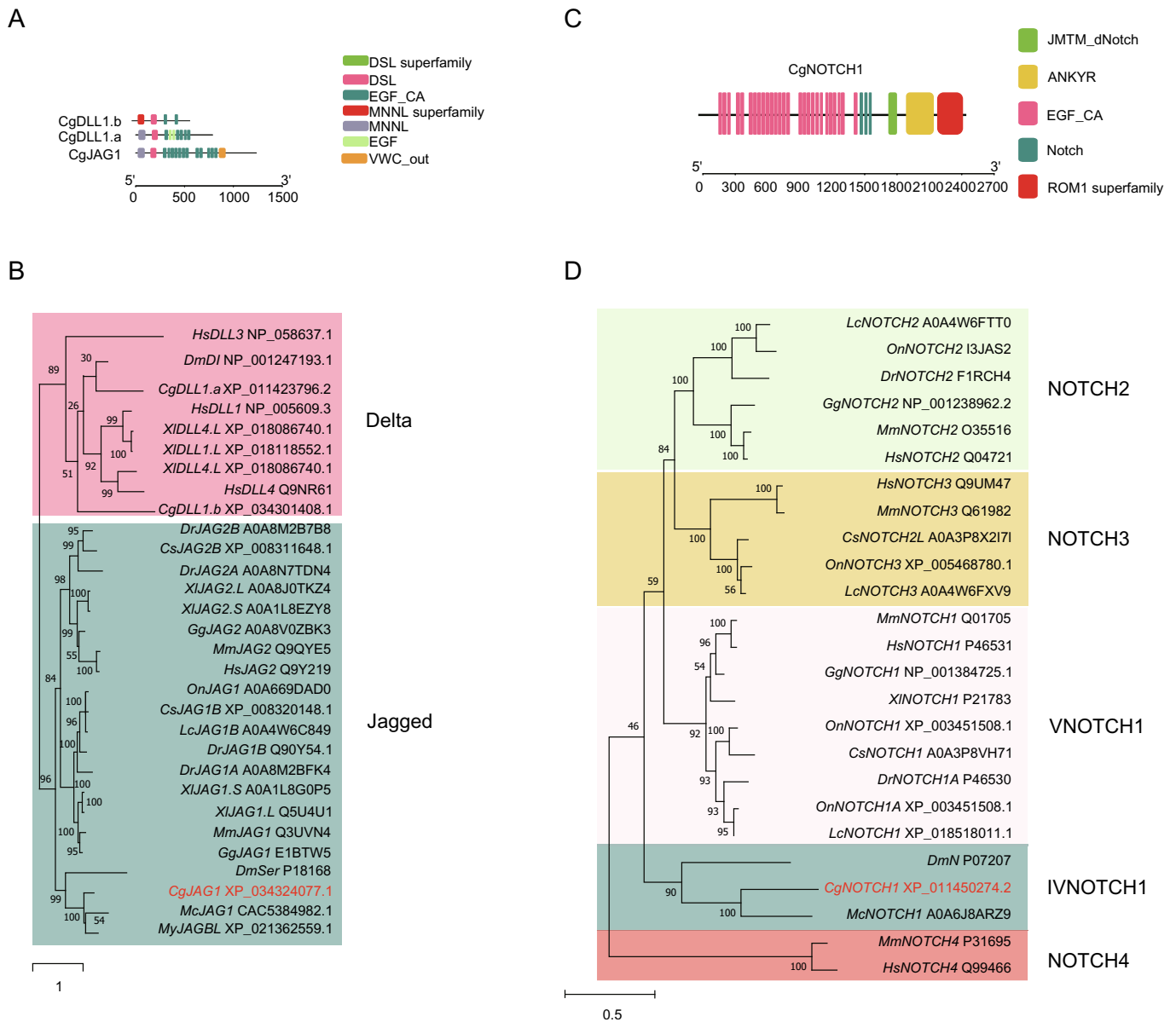


Fig. 2. Sequence structure and phylogenetics analysis of Delta genes and *CgNOTCH1*. (A) Schematic of Delta genes. EGF repeat, DSL, MNNL, and VWC_out domains were predicted. (B) Phylogenetic tree based on the amino acid sequences of Delta genes. Numbers at the nodes indicate the percentage frequencies in 1000 bootstrap replications. The GenBank or Uniprot accession numbers of the sequences follow the name of the species. The pink module indicates the Delta group and the cyan module indicates Jagged clade. *CgJAG1* is noted. (C) Scheme of *CgNOTCH1*. EGF repeat, Notch, ANKYR, and ROM1 domains were identified. (D) Phylogenetic tree of *CgNOTCH1* with amino acid sequences from other species. The green module indicates the NOTCH2 clade, the yellow module indicates NOTCH3 clade, the light pink module indicates the vertebrate NOTCH1 (VNOTCH1) clade, the cyan module indicates the invertebrate NOTCH1 (IVNOTCH1) clade, and the pink module indicates the NOTCH4 clade. (For interpretation of the references to colour in this figure legend, the reader is referred to the web version of this article.)

be situated in the cytoplasm or nucleus (Table S2).

3.3. Developmental and organizational expression patterns of members in Notch signaling pathway

To investigate the potential involvement of Notch pathway members in the development and maintenance of the oyster gonadal microenvironment, we examined the expression patterns of these genes using available transcriptomic data from various oyster tissues. We focused on Delta ligands and conducted a heatmap analysis, which revealed that *CgDLL1.a* and *CgJAG1* exhibited high expression in the gonads (Fig. 4A). Specifically, *CgJAG1* relatively highly expressed in M2n1, although the difference was not statistically significant (Fig. 4A, further illustrated in Fig. S4). Validation via qPCR revealed predominant expression of

CgJAG1 mRNA in male gonads during gametogenesis, with a significant upregulation observed during stage I and II (Fig. 4B). Furthermore, single-cell RNA-seq analysis of oyster gonads during the early stage indicated the specific expression of *CgJAG1* in male niche cells (Wang et al., 2024).

CgNOTCH1 mRNA transcripts was detectable in various tissues, but its expression was significantly higher in mature female gonads (Fig. 4B). In contrast, the qPCR results for *CgSuh* did not show any significant difference in its expression across tissues (Fig. 4B). However, the expression pattern of *CgSuh* varied at different stages of gonadal development. In females, *CgSuh* expression increased progressively with gonadal development, while in males, *CgSuh* expression show no significant variation (Fig. 4B). The expression level of *CgSuh* was significantly lower in triploids compared to diploid mature females (Fig. 4B).

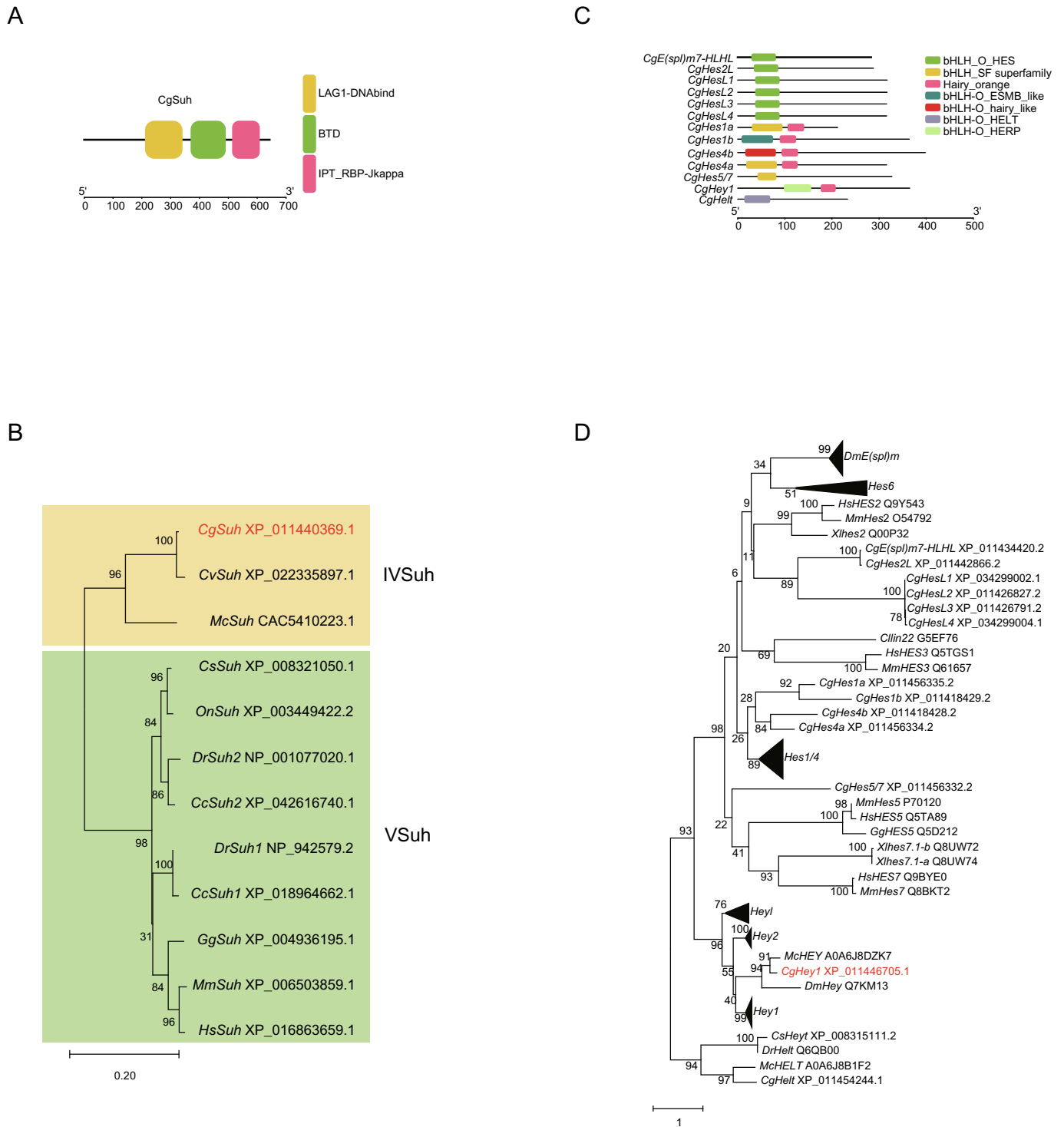


Fig. 3. Sequence structure, phylogenetics, and expression analysis of *CgSuh* and Hes/Hey gene family. (A) Scheme of *CgSuh*. LAG1 DNAbind, BTB, and IPT_RBP Jkappa domains were identified. (B) Phylogenetic tree based on the amino acid sequences of *CgSuh*. The yellow module indicates the invertebrate Suh (IVSuh), and the green indicates the vertebrate Suh (VSuh). (C) Scheme of Hes/Hey genes of *C. gigas*. bHLH and orange domains were identified. (D) Phylogenetic tree of the Hes/Hey genes. Folded evolutionary trees represent target genes from other species (data not shown). (For interpretation of the references to colour in this figure legend, the reader is referred to the web version of this article.)

To identify potential target genes involved in the gonadal microenvironment, we focused on *CgHey1*, which exhibited higher expression levels in male and female gonads (Fig. 4A). Additionally, the heatmap analysis of different gonad stages in diploids revealed that *CgHey1* had higher expression level in stage 1 of males and stage 3 of females (Fig. 4A). We further validated these findings by qPCR (Fig. 4B).

3.4. Spatial expression pattern of *CgJAG1* and *CgNOTCH1*

To manifest whether the ligands and receptors we screened have the potential to interact, we initially constructed the docking model for the interaction between *CgJAG1* and *CgNOTCH1* proteins, which had a high confidence score of 0.8719. (Fig. 5A). However, the confidence score of the docking models for the interaction between *CgDLL1.a* and *CgDLL1*.

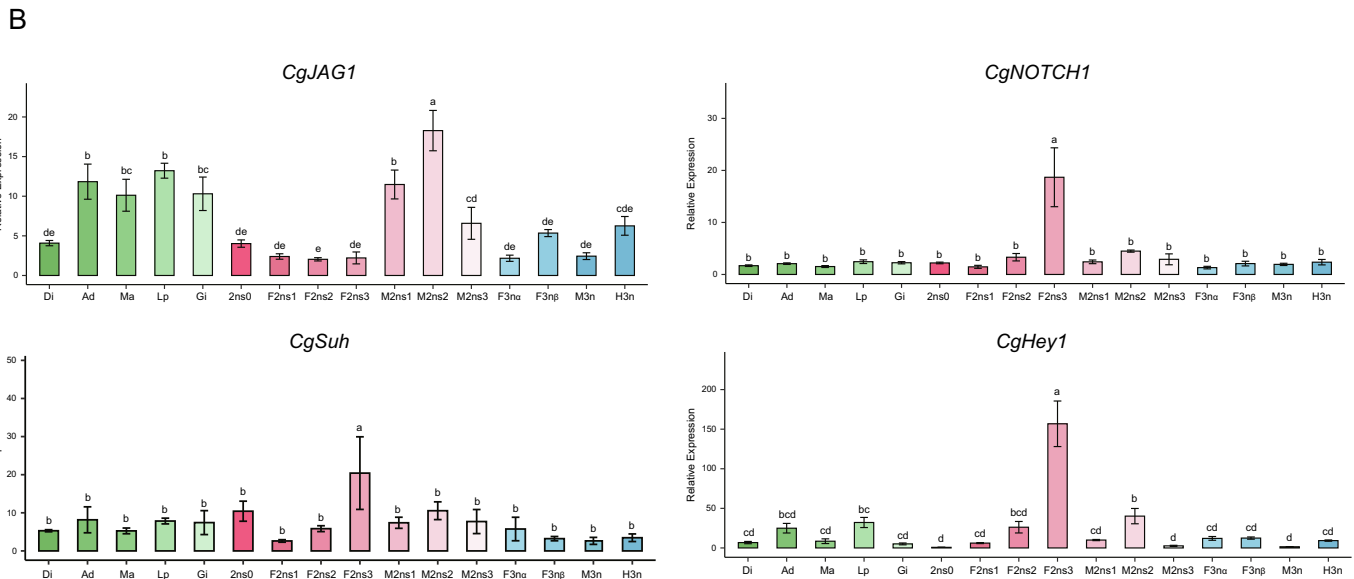
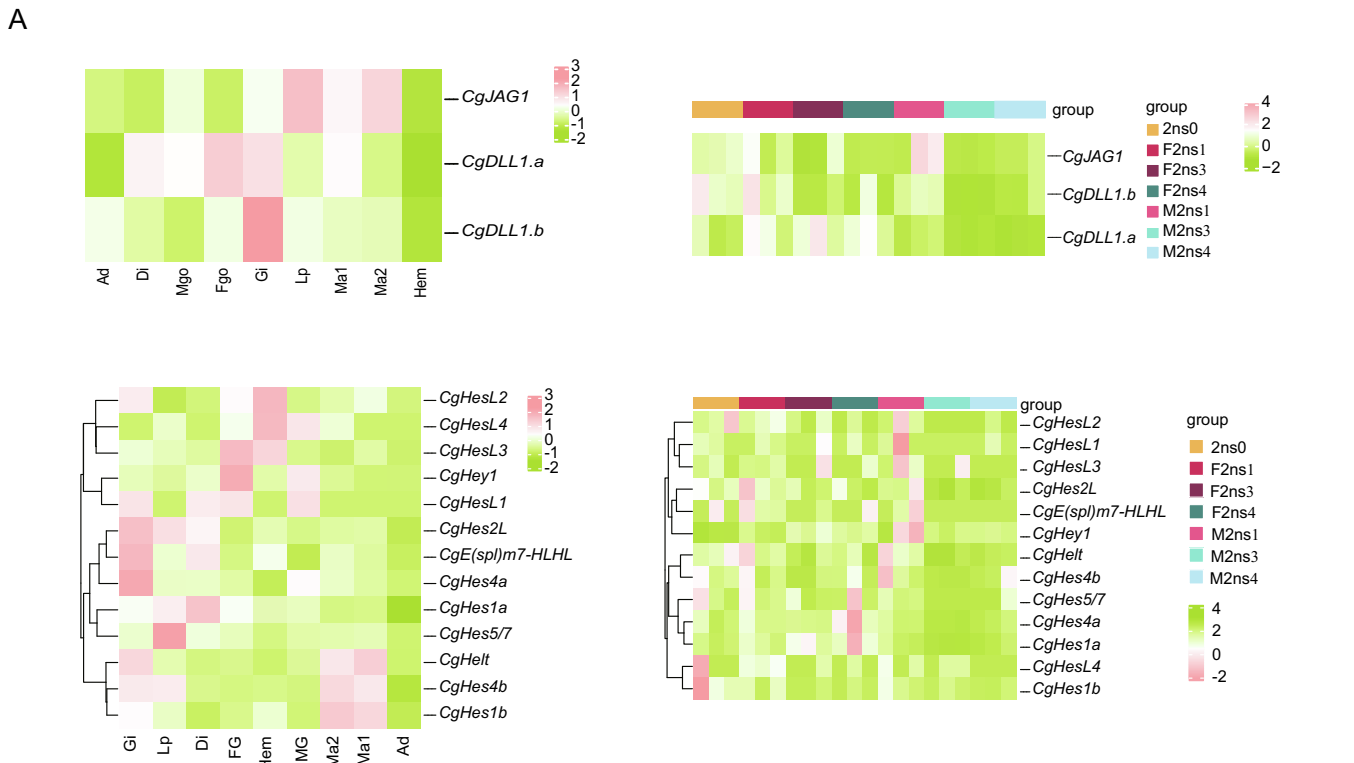


Fig. 4. Expression analysis of NOTCH pathway members. (A) Gene expression heatmap of the Delta genes and Hes/Hey genes in the tissue transcriptome (right) and the gonadal developmental transcriptome (left). Colour indicates mRNA expression levels (TPM). (B) Expression analysis of the *CgJAG1*, *CgNOTCH1*, *CgSuh*, and *CgHey1* estimated by qPCR. Different letters above the error bars indicate significant differences ($P < 0.05$). The green column indicates tissue, the pink column indicates different stages of the diploid gonads, and the blue column indicates triploid gonads. All data are displayed as mean \pm standard error (SE) ($n \geq 3$). Ad, Adductor muscle; Di, Digest; Ma1, Outer edge of mantle; Ma2, Inner part of mantle; Ma, Mantle; Lp, Labial pad; Gi, Gill; Hem, Hemocyte; 2 ns0: Resting period; F2ns1, Proliferating stage of female diploids; F2ns2, Growth stage of female diploids; F2ns3, Ripe stage of female diploids; F2ns4, Spawning stage of female diploids; M2ns1, Proliferating stage of male diploids; M2ns2, Growth stage of male diploids; M2ns3, Ripe stage of male diploids; M2ns4: Spawning stage of male diploids; F3n α , α female triploids; F3n β , β female triploids; M3n α , α male triploids; H3n, Hermaphrodite triploids. (For interpretation of the references to colour in this figure legend, the reader is referred to the web version of this article.)

b, and *CgNOTCH1* were 0.69 and 0.68, respectively (Fig. S3). Subsequently, we examined the spatial expression patterns of *CgJAG1* and *CgNOTCH1* transcripts in oyster gonads. Specifically, we examined the expression pattern of *CgJAG1* in the male gonad during active gametogenesis and at maturity. *In situ* hybridization revealed predominant expression in niche cells, with no expression observed in spermatogonia, spermatocytes, and spermatids (Fig. 5B, C). For *CgNOTCH1*, it was not

detected in the male and female gonadal tubules during early stages (Fig. 5D, F). However, in the mature male gonad, *CgNOTCH1* mRNA expression was primarily found in spermatogonia and spermatocytes, which were situated at the relative lateral margins within the gonadal tubules (Fig. 5E). In the mature ovary, *CgNOTCH1* mRNA expression was detected in the vitellogenic oocytes and the female niche cells (Fig. 5G).

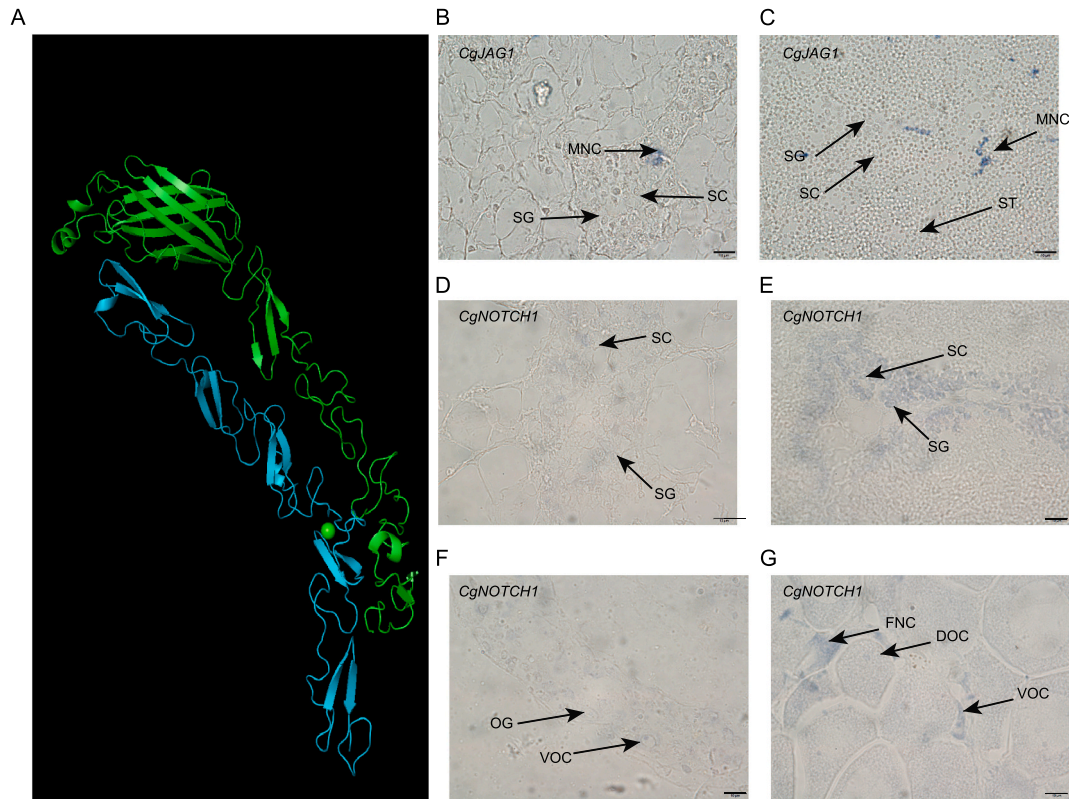


Fig. 5. The spatial pattern of *CgJAG1* and *CgNOTCH1* mRNA localization during male and female gonadal development. (A) Protein model of *CgJAG1* and *CgNOTCH1* binding. The green model indicated *CgJAG1* and the blue model indicated *CgNOTCH1*. The confidence value is 0.8719. Note the intense signal of *CgJAG1* in the male niche cell (MNC) in the gonad during gametogenesis (B) and the gonad at maturity (C). No signal in spermatogonia (SG), spermatocytes (SC), and spermatids (ST). Localization of *CgNOTCH1* with antisense probe in the male gonads during gametogenesis (D) and the gonad at maturity (E), and in the female gonads during gametogenesis (F) and the gonad at maturity (G). Scale bar: 10 μm . (For interpretation of the references to colour in this figure legend, the reader is referred to the web version of this article.)

4. Discussion

Gametogenesis is a complex biological process dependent on the proliferation and differentiation of germ cells, as well as the presence of the gonadal niche. Notch signaling is known to play a critical role in the establishment and maintenance of the gonadal niche. This study aimed to characterize the gonadal niche of the oyster and identify the Notch pathway components that may be involved in the oyster gonadal niche.

In our observation, we found somatic cells within acini alongside male and female germ cells. In mammals, amphibians, fish, and insect, somatic cells in cyst, an extreme evolutionary conservation, usually is in contact only with a single germ cell clone (Leal et al., 2009; Spradling, 2024). Our results together with those of the previous research showed that at all stages of gametogenesis (except spermatozoon), a group of niche cells surrounding the germ cells in Pacific oysters (Franco et al., 2011). In the male gonads, spermatogenic cells were found interspersed with substantial “empty space”, which was filled by niche cells rich in vacuoles. These findings align well with previous studies that have characterized the morphology of male niche cells during the reproductive cycle (Franco et al., 2011). Moreover, the fine structure of male niche cells in *C. gigas* resembles that of other bivalve mollusks such as *Calyptogena pacifica* (Yurchenko et al., 2022), *Modiolus kurilensis* (Yurchenko and Vaschenko, 2010), *Pitar rudis* and *Chamelea gallina* (Erkan and Sousa, 2002). A more detailed characterization of the two types male niche cells could contribute to a better understanding the diversity of oyster niches (Kim et al., 2010). The formation of single-membrane phagolysosomes at different stages suggests that these niche cells might be in degrading contents, potentially including defective or residual germ cells (Erkan and Sousa, 2002). Niche cells are known to accumulate and transfer nutrients, and thus, the high glycogen

content in niche cells may play a role in providing energy during spermatogenesis (Yurchenko et al., 2022). Notably, the TEM data highlights differences in the morphology of testes niche cells compared to ovarian niche cells. Female niche cells attach to oocytes or oogonia in a wedge pattern and exhibit rough endoplasmic reticulum along with glycogen-rich granules. As discussed earlier, this distinct morphology suggests that female niche cells are likely involved in the heterosynthetic process of yolk formation (Eckelbarger and Hodgson, 2021). Thus, we propose that the sexual morphological differences in niche cells may be attributed to their distinct roles in the microenvironment of male and female gonads.

Desmosomes play a crucial role in mediating cell-cell adhesion, both between opposing cells (trans conformation) and on the same cell surface (cis conformation). These desmosomes are essential for germ cell survival and sex differentiation (Piprek et al., 2017; Shafraz et al., 2018). In line with previous studies on mollusks, we observed intercellular desmosome-like junctions between niche cells and germ cells, as well as between adjacent niche cells (Yurchenko et al., 2022; Yurchenko and Vaschenko, 2010). The presence of desmosome-like connections between niche cells and germ cells suggests strong adhesion between these cells, potentially aiding in the support and protection of germ cells within the niche. Our immunohistochemistry assay did not yield positive results in the gonads, probably due to the unsuitability of the primary antibody used. Extensive studies on mammals have shown that cell-cell contact between niche cells forms the blood-testis barrier (BTB), which protects post-meiotic germ cells from the systemic circulation (Kopera et al., 2010). The disruption of niche cell function in oysters leads to gonadal sterility, accompanied by the filling of the gonadal tubules with hemocytes (Huvet et al., 2012). Therefore, we speculate that the formation of desmosome-like connection between

niche cells contributes to the protective barrier for germ cells. Overall, the presence of these connections indicates that oyster gonads are not simply a collection of isolated cells, but rather a complex, organized system where cells can interact and communicate with each other.

The physical approximation of niche cells with germ cells is crucial for signaling and determining cell fate during gametogenesis (McGinnis et al., 2013). One well-studied example is the case of Notch. Notch signaling has been found to maintain Leydig progenitor cells in the mouse testis, contribute to follicle formation in the human ovary, and regulate meiosis of female germ cells (Feng et al., 2014; Tang et al., 2008; Vanorny and Mayo, 2017). However, the molecular mechanisms and signal transduction of molluscan niche are still unclear. In our study, three ligands (*CgJAG1*, *CgDLL1.a*, and *CgDLL1.b*) and one receptor (*CgNOTCH1*) were identified in oyster. Extracellular interactions, mediated by Delta ligands and Notch receptors, are based on several conserved domains (Borggreve and Oswald, 2009). The EGF repeats were found in both ligands and the receptor of oyster. Additionally, Notch repeat (specific for receptors) and DSL domain (specific for ligands) were found in our study. Furthermore, *CgJAG1* and *CgNOTCH1* were found to be closer to *DmSer* and *DmN*, suggesting similarly important role in regulating niche formation (Kitadate and Kobayashi, 2010). In our study, the expression level of *CgJAG1* was significantly higher during active gametogenesis in diploid testes. In contrast to findings in other species, our data showed strong positivity *CgJAG1* in a cluster of cells in the male germ cells gap. Based on their morphology and location, these cluster of cells may represent male niche cells. Additionally, spermatogonia and spermatocytes exhibited positivity for *CgNOTCH1* (Trombly et al., 2009; Xu and Gridley, 2013). This suggests that niche cells may play a role in oyster germ cell proliferation and differentiation. The high expression level of *CgNOTCH1* in vitellogenic oocytes and female niche cells indicated its role in follicle histogenesis (Vanorny and Mayo, 2017).

The *Suh* gene serves as a transcriptional mediator of Notch. *CgSuh* contains the IPT_RBP-Jkappa domain, considered essential when combined with the Notch Intracellular Domain (NICD) (Artavanis-Tsakonas et al., 1995). *Suh* has been reported to play a role in gonadal differentiation of Yellow River carp (Jia et al., 2018). The nonsignificant differential expression of *CgSuh* in multiple tissues implies a wide range of roles in the different tissues in oysters. In our study, Hairy and enhancer of split (Hes) and Hes-related YRPW motif TF (Hey), identified as primary target genes of the Notch signaling pathway, were also identified. We specifically focused on *CgHey1* due to its high expression in gonadal tissue. *CgHey1* was found to possess conserved domains, including the helix-loop-helix domain and Orange domain (Iso et al., 2003). *CgHey1* and *DmHey* were closely grouped together, indicating a similar function in cell fate determination (Mark et al., 2021).

5. Conclusion

In this study, desmosome-like connections were observed between niche cells and germ cells, as well as between adjacent niche cells, in both male and female gonads. The members of the Notch signaling pathway potentially involved in coordinated gonadal communication were also identified. *CgJAG1* and *CgNOTCH1* were spatially expressed in niche cells and germ cells, respectively, within the male gonad. These findings demonstrate the important role of the Notch signaling pathway in the gonadal niche of oysters.

CRedit authorship contribution statement

Huihui Wang: Writing – original draft, Software, Methodology, Formal analysis. **Hong Yu:** Writing – review & editing, Writing – original draft, Validation, Methodology. **Qi Li:** Writing – review & editing.

Declaration of competing interest

The authors declare that they have no known competing financial interests or personal relationships that could have appeared to influence the work reported in this paper.

Data availability

Data will be made available on request.

Acknowledgements

This study was supported by grants from National Natural Science Foundation of China (42276111) and Science Foundation of Shandong Province (ZR2022MC171).

Appendix A. Supplementary data

Supplementary data to this article can be found online at <https://doi.org/10.1016/j.cbpa.2024.111639>.

References

- Almagro Armenteros, J.J., Tsirigos, K.D., Sønderby, C.K., Petersen, T.N., Winther, O., Brunak, S., von Heijne, G., Nielsen, H., 2019. SignalP 5.0 improves signal peptide predictions using deep neural networks. *Nat. Biotechnol.* 37, 420–423. <https://doi.org/10.1038/s41587-019-0036-z>.
- Artavanis-Tsakonas, S., Matsuno, K., Fortini, M.E., 1995. Notch signaling. *Science* 268, 225–232. <https://doi.org/10.1126/science.7716513>.
- Borggreve, T., Oswald, F., 2009. The notch signaling pathway: transcriptional regulation at notch target genes. *Cell. Mol. Life Sci.* 66, 1631–1646. <https://doi.org/10.1007/s00018-009-8668-7>.
- Chou, K.-C., Shen, H.-B., 2010. A new method for predicting the subcellular localization of eukaryotic proteins with both single and multiple sites: Euk-mPLoc 2.0. *PLoS One* 5, e9931. <https://doi.org/10.1371/journal.pone.0009931>.
- Eckelbarger, K.J., Hodgson, A.N., 2021. Invertebrate oogenesis - a review and synthesis: comparative ovarian morphology, accessory cell function and the origins of yolk precursors. *Invertebr. Reprod. Dev.* 65, 71–140. <https://doi.org/10.1080/07924259.2021.1927861>.
- Erkan, M., Sousa, M., 2002. Fine structural study of the spermatogenic cycle in *Pitar rudis* and *Chamelea gallina* (Mollusca, Bivalvia, Veneridae). *Tissue Cell* 34, 262–272. [https://doi.org/10.1016/S0040-8166\(02\)00016-2](https://doi.org/10.1016/S0040-8166(02)00016-2).
- Farcy, É., Voiseux, C., Lebel, J.-M., Fiévet, B., 2009. Transcriptional expression levels of cell stress marker genes in the Pacific oyster *Crassostrea gigas* exposed to acute thermal stress. *Cell Stress Chaperones* 14, 371. <https://doi.org/10.1007/s12192-008-0091-8>.
- Feng, Y.-M., Liang, G.-J., Pan, B., Qin, X., Zhang, X.-F., Chen, C.-L., Li, L., Cheng, S.-F., De Felici, M., Shen, W., 2014. Notch pathway regulates female germ cell meiosis progression and early oogenesis events in fetal mouse. *Cell Cycle* 13, 782–791. <https://doi.org/10.4161/cc.27708>.
- Franco, A., Kellner, K., Goux, D., Mathieu, M., Heude Berthelin, C., 2011. Intra-gonadal somatic cells (ISCs) in the male oyster *Crassostrea gigas*: morphology and contribution in germinal epithelium structure. *Micron* 42, 718–725. <https://doi.org/10.1016/j.micron.2011.04.003>.
- Huvet, A., Fleury, E., Corporeau, C., Quillien, V., Daniel, J.Y., Riviere, G., Boudry, P., Fabioux, C., 2012. In vivo RNA interference of a gonad-specific transforming growth factor-β in the Pacific oyster *Crassostrea gigas*. *Mar. Biotechnol.* 14, 402–410. <https://doi.org/10.1007/s10126-011-9421-4>.
- Iso, T., Kedes, L., Hamamori, Y., 2003. HES and HERP families: multiple effectors of the notch signaling pathway. *J. Cell. Physiol.* 194, 237–255. <https://doi.org/10.1002/jcp.10208>.
- Jia, Y., Wang, F., Zhang, R., Liang, T., Zhang, W., Ji, X., Du, Q., Chang, Z., 2018. Identification of *suh* gene and evidence for involvement of notch signaling pathway on gonadal differentiation of Yellow River carp (*Cyprinus carpio*). *Fish Physiol. Biochem.* 44, 375–386. <https://doi.org/10.1007/s10695-017-0441-5>.
- Katoh, K., Standley, D.M., 2013. MAFFT multiple sequence alignment software version 7: improvements in performance and usability. *Mol. Biol. Evol.* 30, 772–780. <https://doi.org/10.1093/molbev/mst010>.
- Kiger, A.A., White-Cooper, H., Fuller, M.T., 2000. Somatic support cells restrict germline stem cell self-renewal and promote differentiation. *Nature* 407, 750–754. <https://doi.org/10.1038/35037606>.
- Kim, J.H., Chung, E.-Y., Choi, K.-H., Lee, K.-Y., Choi, M.S., 2010. Ultrastructure of the Testis and Germ Cell Development during Spermatogenesis in Male *Crassostrea gigas* (Bivalvia: Ostreidae) in Western Korea.
- Kitadate, Y., Kobayashi, S., 2010. Notch and Egfr signaling act antagonistically to regulate germ-line stem cell niche formation in *Drosophila* male embryonic gonads. *Proc. Natl. Acad. Sci.* 107, 14241–14246. <https://doi.org/10.1073/pnas.1003462107>.

- Kopera, I.A., Bilinska, B., Cheng, C.Y., Mruk, D.D., 2010. Sertoli-germ cell junctions in the testis: a review of recent data. *Philos. Trans. R. Soc. B* 365, 1593–1605. <https://doi.org/10.1098/rstb.2009.0251>.
- Leal, M.C., Cardoso, E.R., Nóbrega, R.H., Batlouni, S.R., Bogerd, J., França, L.R., Schulz, R.W., 2009. Histological and stereological evaluation of zebrafish (*Danio rerio*) spermatogenesis with an emphasis on Spermatogonial Generations1. *Biol. Reprod.* 81, 177–187. <https://doi.org/10.1095/biolreprod.109.076299>.
- Li, L., Dong, J., Yan, L., Yong, J., Liu, X., Hu, Y., Fan, X., Wu, X., Guo, H., Wang, X., Zhu, X., Li, R., Yan, J., Wei, Y., Zhao, Y., Wang, W., Ren, Y., Yuan, P., Yan, Z., Hu, B., Guo, F., Wen, L., Tang, F., Qiao, J., 2017. Single-cell RNA-seq analysis maps development of human germline cells and gonadal niche interactions. *Cell Stem Cell* 20, 858–873.e4. <https://doi.org/10.1016/j.stem.2017.03.007>.
- Li, Z., Li, Q., Xu, C., Yu, H., 2022. Molecular characterization of *Pax7* and its role in melanin synthesis in *Crassostrea gigas*. *Comp. Biochem. Physiol. B: Biochem. Mol. Biol.* 260, 110720 <https://doi.org/10.1016/j.cbpb.2022.110720>.
- Mark, B., Lai, S.-L., Zarin, A.A., Manning, L., Pollington, H.Q., Litwin-Kumar, A., Cardona, A., Truman, J.W., Doe, C.Q., 2021. A developmental framework linking neurogenesis and circuit formation in the *Drosophila* CNS. *eLife* 10, e67510. <https://doi.org/10.7554/eLife.67510>.
- Mazzoni, T.S., Grier, H.J., Quagio-Grassiotto, I., 2010. Germline cysts and the formation of the germinal epithelium during the female gonadal morphogenesis in *Cyprinus carpio* (Teleostei: Ostariophysi: Cypriniformes). *Anat. Rec.* 293, 1581–1606. <https://doi.org/10.1002/ar.21205>.
- McGinnis, L.K., Limback, S.D., Albertini, D.F., 2013. Signaling modalities during oogenesis in mammals. In: *Current Topics in Developmental Biology*. Elsevier, pp. 227–242. <https://doi.org/10.1016/B978-0-12-416024-8.00008-8>.
- McIntyre, D.C., Nance, J., 2020. Niche cell wrapping ensures primordial germ cell quiescence and protection from intercellular cannibalism. *Curr. Biol.* 30, 708–714.e4. <https://doi.org/10.1016/j.cub.2019.12.021>.
- Piprek, R.P., Kolasa, M., Podkowa, D., Kloc, M., Kubiak, J.Z., 2017. Cell adhesion molecules expression pattern indicates that somatic cells arbitrate gonadal sex of differentiating bipotential fetal mouse gonad. *Mech. Dev.* 147, 17–27. <https://doi.org/10.1016/j.mod.2017.07.001>.
- Shafraz, O., Rübbsam, M., Stahley, S.N., Caldara, A.L., Kowalczyk, A.P., Niessen, C.M., Sivasankar, S., 2018. E-cadherin binds to desmoglein to facilitate desmosome assembly. *eLife* 7, e37629. <https://doi.org/10.7554/eLife.37629>.
- Spradling, A.C., 2024. The ancient origin and function of germline cysts. In: Kloc, M., Uosef, A. (Eds.), *Syncytia: Origin, Structure, and Functions*. Springer International Publishing, Cham, pp. 3–21. https://doi.org/10.1007/978-3-031-37936-9_1.
- Stamatakis, A., 2014. RAxML version 8: a tool for phylogenetic analysis and post-analysis of large phylogenies. *Bioinformatics* 30, 1312–1313. <https://doi.org/10.1093/bioinformatics/btu033>.
- Tang, H., Brennan, J., Karl, J., Hamada, Y., Raetzman, L., Capel, B., 2008. Notch signaling maintains Leydig progenitor cells in the mouse testis. *Development* 135, 3745–3753. <https://doi.org/10.1242/dev.024786>.
- Trombly, D.J., Woodruff, T.K., Mayo, K.E., 2009. Suppression of notch signaling in the neonatal mouse ovary decreases primordial follicle formation. *Endocrinology* 150, 1014–1024. <https://doi.org/10.1210/en.2008-0213>.
- Vanorny, D.A., Mayo, K.E., 2017. The role of notch signaling in the mammalian ovary. *Reproduction (Cambridge, England)* 153, R187. <https://doi.org/10.1530/REP-16-0689>.
- Wang, H., Yu, H., Li, Q., 2024. Integrative analysis of single-nucleus RNA-seq and bulk RNA-seq reveals germline cells development dynamics and niches in the Pacific oyster gonad. *iScience* 0. <https://doi.org/10.1016/j.isci.2024.109499>.
- Xu, J., Gridley, T., 2013. Notch2 is required in somatic cells for breakdown of ovarian germ-cell nests and formation of primordial follicles. *BMC Biol.* 11, 13. <https://doi.org/10.1186/1741-7007-11-13>.
- Yue, C., Li, Q., Yu, H., 2018. Gonad transcriptome analysis of the Pacific oyster *Crassostrea gigas* identifies potential genes regulating the sex determination and differentiation process. *Mar. Biotechnol.* 20, 206–219. <https://doi.org/10.1007/s10126-018-9798-4>.
- Yue, C., Li, Q., Yu, H., 2021. Variance in expression and localization of sex-related genes *CgDsx*, *CgBHMGI* and *CgFoxl2* during diploid and triploid Pacific oyster *Crassostrea gigas* gonad differentiation. *Gene* 790, 145692. <https://doi.org/10.1016/j.gene.2021.145692>.
- Yurchenko, O.V., Vaschenko, M.A., 2010. Morphology of spermatogenic and accessory cells in the mussel *Modiolus kurilensis* under environmental pollution. *Mar. Environ. Res.* 70, 171–180. <https://doi.org/10.1016/j.marenvres.2010.04.007>.
- Yurchenko, O.V., Borzykh, O.G., Kalachev, A.V., 2022. Microscopic anatomy of gonadal area in the deep-sea clam *Calyptogena pacifica* (Bivalvia: Vesicomidae) with emphasis on somatic cells. *Tissue Cell* 75, 101743. <https://doi.org/10.1016/j.tice.2022.101743>.